A Transparent Conductive Adhesive Laminate Electrode for High-Efficiency Organic-Inorganic Lead Halide Perovskite Solar Cells

*Daniel Bryant, Peter Greenwood, Joel Troughton, Maarten Wijdekop, Mathew Carnie, Matthew Davies, Konrad Wojciechowski, Henry J. Snaith, Trystan Watson, and David Worsley**

A key challenge that can unlock the potential of third generation photovoltaics (PV) is the development of low cost indium free flexible transparent electrodes to enable lightweight, transparent and metal mounted devices. Here we describe a major breakthrough which allows a highly conducting self-adhesive laminate electrode to be applied to devices at room temperature which could be applied to scale up flexible lightweight PV applications. The development of solid state organic-inorganic metal halide perovskite solar cells (PSCs)[1–3] with over 15% efficiency at lab-scale devices is extraordinarily exciting for third generation PV technology since it offers efficiency values comparable to conventional and commercial PV.[4] Key to PSCs not merely being a lab curiosity is solving certain manufacturing processes required to scale these lab devices into modules.[5] Typically laboratory charge collection at the counter electrode is achieved via evaporation of an opaque gold metallic contact onto the active material. Whilst being a very effective ohmic contact, it limits the potential for commercial manufacture given the expense and opacity of the gold which would prevent the application of perovskites for transparent or metal mounted applications. In this work we have developed a novel semi-transparent electrode design combining a polymer embedded nickel grid with a transparent conducting contact adhesive that can be applied to perovskite based devices providing conductivity, charge extraction, mechanical adhesion and protection. This has allowed indium-tin oxide (ITO), Au and Ag free entirely non-vacuum processed PSC devices to be fabricated with a solar-to-electrical power conversion efficiency (PCE) of over 15%.

There are some excellent alternatives to replace thermally evaporated silver and gold electrodes in third generation photovoltaic devices, such as solid-state Dye Sensitized Solar Cells (s-DSC) and Organic Photovoltaics (OPV) based on the use of solution processed silver nanowires.[6–8] In these situations comparable performance has been achieved to vapor deposited electrodes. Prior to these developments, nanoparticulate silver inks deposited onto the photovoltaic (PV) devices with subsequent heating of the whole device to 150–200 °C were a route to applying the conductor via printing.[9] This can cause degradation of temperature sensitive components within the devices, such as the hole transporter which is commonly used (Spiro-OMeTAD) with a resultant loss of PV performance. Silver nanowires are advantageous in this respect as the heating step to anneal the nanowires can be conducted separately before being applied onto the devices at room temperature. This is due to the nanowire mesh's low sheet resistance and a good electrical contact made with the cells.[6] There are however issues with the use of silver based conductors in contact with the PSC since the halide content can give rise to silver halide formation and degradation of performance and we sought a different solution for PSCs.

The currently reported high efficiencies of 12–15% for PSCs have been achieved with a vapor deposited precious metal contact (usually gold). Silver based coatings could suffer from degradation through the formation of silver halides leading to a contact breakdown with the Spiro-OMeTAD.[10] In order to develop an indium and precious metal free transparent conductor we have combined a corrosion proof Ni mesh electrode (embedded in a PET film) with a silver-free transparent conducting adhesive (TCA). The whole electrode can be fabricated separately to the organic-inorganic lead halide perovskite photoelectrode and then simply laminated at room temperature.

The transparent electrode material was obtained from Epigem and is a Ni mesh embedded in a PET film on a roll to roll process; this produces a robust and highly conductive electrode at less than half the cost of ITO PET. The mesh spacing is *ca* 300 µm, and the PET film with the mesh is 86% transparent and is shown in **Figure 1**a. The mesh electrode has extremely

D. Bryant, P. Greenwood, J. Troughton, Dr. M. Carnie, Dr. M. Davies, Dr. T. Watson, Prof. D. Worsley
SPECIFIC, College of Engineering
Swansea University
Baglan Bay Innovation and Knowledge Centre
Central Avenue
Baglan, SA12 7AX, UK
E-mail: d.a.worsley@swansea.ac.uk

Dr. M. Wijdekop
Centre for Process Innovation Limited (CPI)
National Printable Electronics Centre
NETPark, Sedgefield, County Durham TS21 3FG, UK

K. Wojciechowski, Prof. H. J. Snaith
Photovoltaic and Optoelectronic Device Group
Department of Physics
Oxford University, UK

DOI: 10.1002/adma.201403939

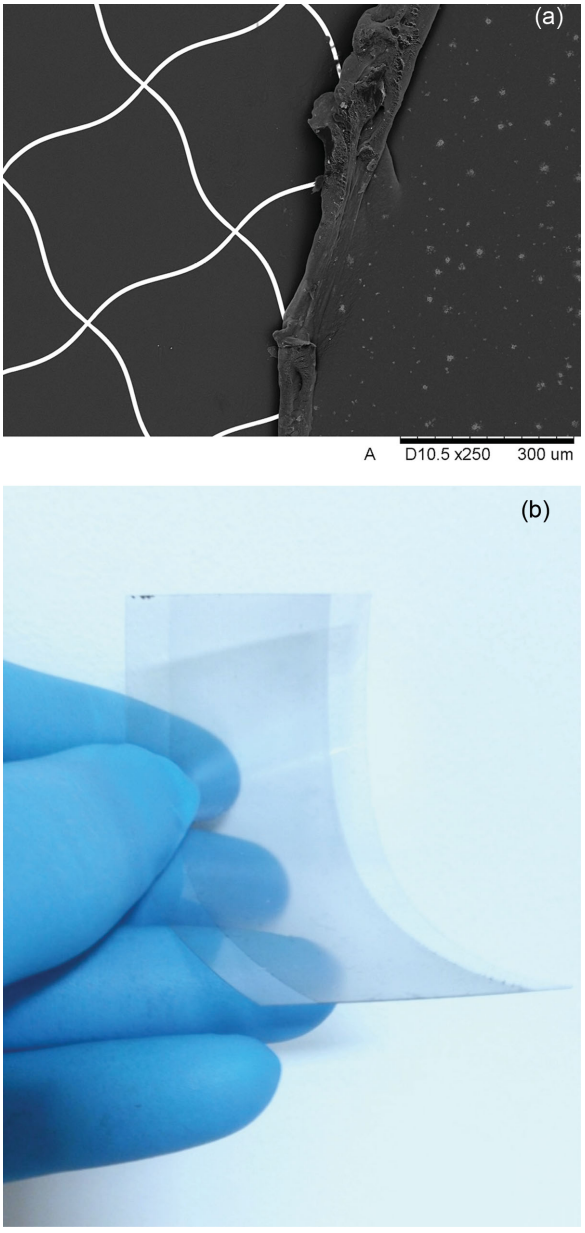

Figure 1. (a) SEM micrograph of transparent conducting adhesive (TCA) applied to an embedded Ni grid on PET (Epigem) (b) Photo of the TCA-Laminate transparent counter electrode incorporating the metal mesh.

attractive large area lateral conductivity of ca 1.2 Ω sq^{-1}. In order to get an electrical contact and hole extraction from the perovskite active layer, this is coated with the TCA (shown in finished form in Figure 1b). The TCA is specifically designed to have extremely high transparency and conduction paths vertically (*z*-conduction) between the perovskite and the Ni counter electrode wires. In addition, the TCA is a pressure sensitive adhesive therefore no heating step is required for activation and application. To achieve conduction in the adhesive we chose to use commercially available PEDOT:PSS as it is a widely used conducting polymer that provides conductivity while maintaining transparency and has been shown to be compatible with perovskite based devices.[11–14]

Figure 2 illustrates the schematic cross section of the PSC devices in this work and the target thicknesses. In this architecture we have used a similar approach to that described recently[15] for SSDSC with a silver nano wire/PEDOT:PSS electrode. In other words a Spiro-OMeTAD layer is applied to the active perovskite layer and then PEDOT:PSS is used as the electrical contact. In our architecture we have used a PEDOT:PSS interlayer on the Spiro-OMeTAD to ensure good electrical contact with the PEDOT:PSS adhesive and metal grid electrode as the adhesive itself has only a small quantity of the conductor as will be demonstrated. The 'dry' PEDOT:PSS used in this work was specifically chosen as it has a minimal water content. The solution is made using alcohols and the water content is solely that which cannot be distilled from the solvent system. In our case this is based on propylene glycol and as such the water content is under 3%. In these conditions we (and others[15]) have found that the underlying Spiro-OMeTAD is unaffected. This is particularly important in this study since water would damage the underlying perovskite active layer.

To create the TCA we blended the PEDOT:PSS with an acrylic adhesive. An acrylic micro-emulsion was selected as the adhesive phase for several reasons. Firstly the micro-emulsion adhesive and PEDOT:PSS are both aqueous compatible which makes them easy to mix. The adhesive has a high degree of transparency when cured, >98%, (Figure S1), which is desirable for reverse illuminated cells such as those processed on metal foils. The cured adhesive achieves and maintains mechanical contact with substrates through pressure sensitive adhesion and has zero water content so does not create issues with either the perovskite or Spiro-OMeTAD. Arguably the most important aspect of the dual phase approach is that the micro-emulsion of the adhesive enables phase segregation between PEDOT:PSS and the polymer adhesive domains, which is advantageous for achieving conductivity well below a conventional percolation threshold.

Figure 3a outlines the desired structure within the TCA with the adhesive forcing the segregation of the conducting polymer phase. Figure 3b shows the effect of the variation of volume fraction of the PEDOT:PSS in the adhesive dried film in which it can be seen that the conductivity of the layer becomes significant at very low volume fraction PEDOT:PSS additions ($\phi < 0.02$). In **Figure 4** a cryogenically sliced atomic force microscopy (AFM) image of the TCA (PEDOT:PSS phase appears as lighter regions) shows that the PEDOT:PSS is distributed in a honeycomb arrangement around the larger 150 nm domains typical of the acrylic emulsion PSA.[16] The PEDOT:PSS regions around the boundaries of these particles are *ca* 60 nm in diameter. It is evidentially this structure that allows a spanning conducting network of PEDOT:PSS to percolate through the TCA at ϕ of 0.0175, more than an order of magnitude lower than $\phi = 0.18$ suggested by percolation theory for randomly distributed spheres.[17] This low φ of the PEDOT:PSS allows the TCA to maintain a transparency of >90% at a wavelength of 500 nm with a dry film thickness of 29 µm, (Figure S1) as well as an adhesive tack value of 29 cm, measured using the tape industry ASTM D3121 standard rolling ball tack (RBT), leaving it within the range of common pressure sensitive adhesive tapes (5–30 cm).[18,19]

The bulk conductivity of the adhesive is an important measurement of the TCA since its primary function will be to conduct in the z-axis. Using a four point probe the bulk conductivity

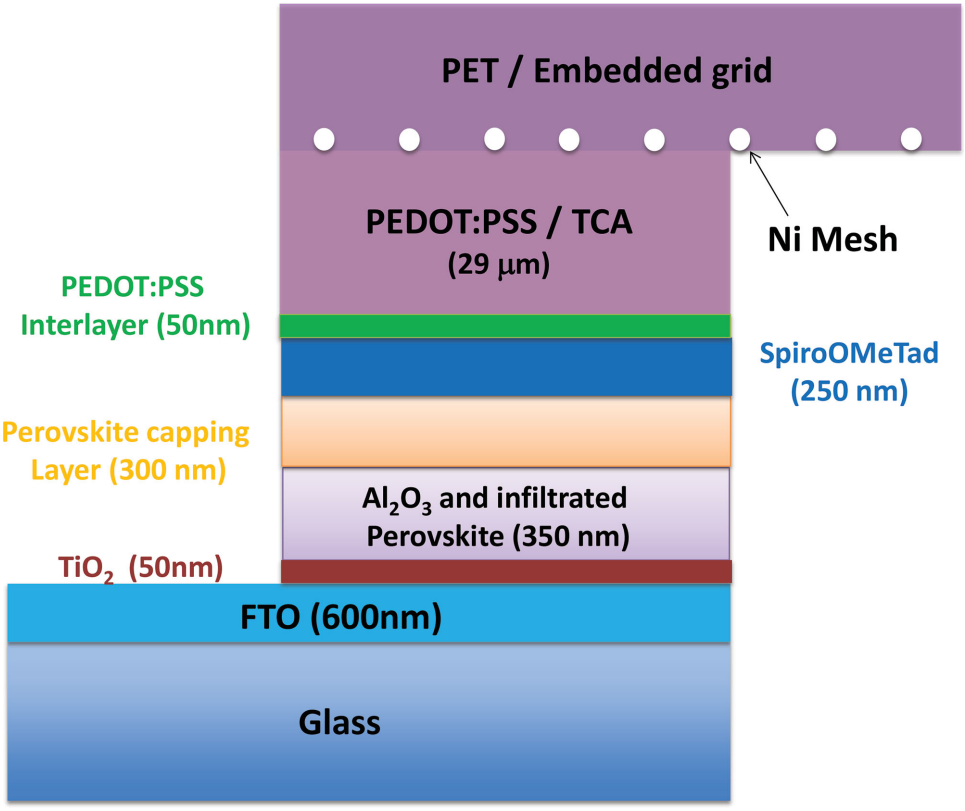

Figure 2. Schematic of PSC layers together with representative target thicknesses.

of the TCA at ϕ of 0.0175 measures 0.11 S cm^{-1}, this is four orders of magnitude higher than doped Spiro-OMeTAD[20] and sufficient for z-axis charge extraction from the devices through the 29 μm thick TCA layer. This conductivity alone is insufficient for bulk charge extraction and would lead to significant resistive losses, therefore a transparent conducting sheet with a low sheet resistance is required in conjunction with the TCA for large area charge extraction from devices in the x-y directions.

To complete the collection electrode in this study a Ni microgrid electrochemically embeddeded into PET was used (Epimesh 300 by EPIGEM see Figure 1a) which has a very low sheet resistance of 1.2 Ω sq^{-1}. The TCA material was applied via doctor blading to the PET microgrid to form a functional laminate (Figure 1b). To test the performance of the TCA-laminate, $CH_3NH_3PbI_{3-x}Cl_x$ mesosuperstructured perovskite solar cells (PSCs) were fabricated as reported elsewhere[3,21] with conventional evaporated gold contacts and with the TCA-laminate applied directly onto the Spiro-OMeTAD p-type charge collection layer with a typical rolling pressure of 50kPa consistent with cold lamination processes.

Initially when the TCA was adhered directly to the Spiro-OMeTAD poor electrical contact was observed which was revealed with high interfacial cell resistances recorded using Electrochemical Impedance Spectroscopy. This initially disappointing result is not surprising given the very low PEDOT:PSS loading in the adhesive (1.75%). The PEDOT:PSS at the surface

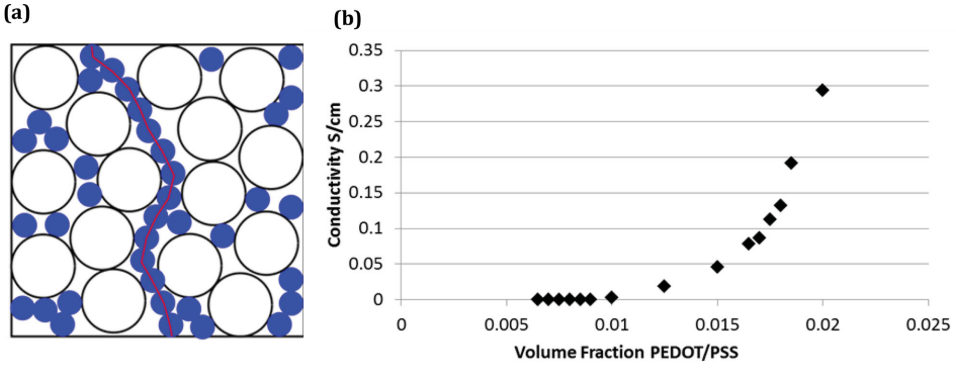

Figure 3. (a) Schematic illustrating ordered percolation; (b) Change in bulk conductivity with the change in volume fraction (ϕ) of PEDOT:PSS in the dry TCA film

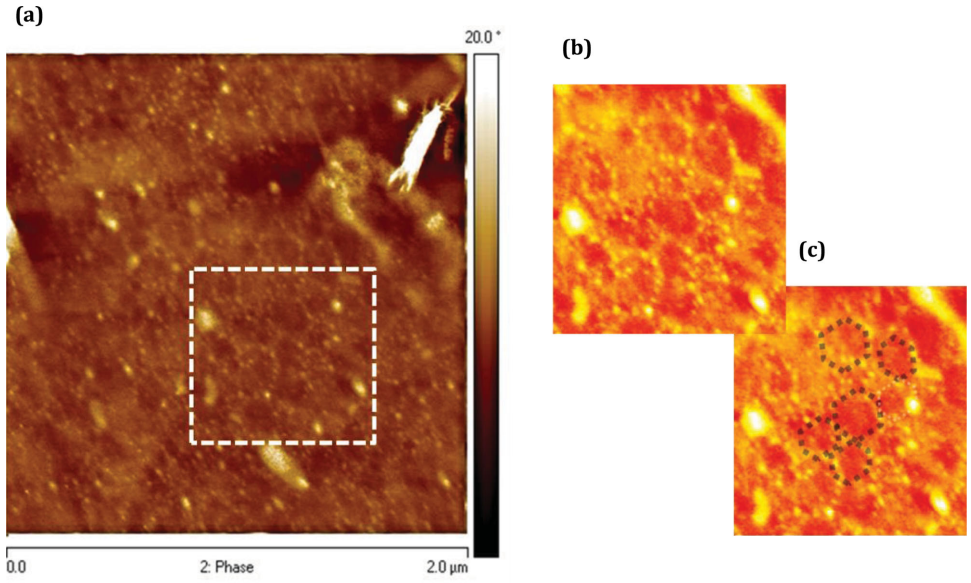

Figure 4. TCA AFM and structure. (a) AFM image of a PSA with a 0.02 ϕ PEDOT:PSS achieved through cryo-slicing. (b) and (c) Contrast enhanced images derived from (a) annotated to demonstrate honeycomb packing

of a TCA containing a PEDOT:PSS ϕ of 0.0175 is at most ~1.75% of the total surface area. As such the PEDOT:PSS is spaced around 200–500 nm apart and, combined with the higher resistivity of Spiro-OMeTAD (3.7 MΩ cm-1), current will only be collected from 1.75% directly under the protruding PEDOT:PSS outcrops and a small region laterally encompassing it. To create an effective contact between the Spiro-OMeTAD and the outcropping PEDOT:PSS and aid lateral charge collection across the whole Spiro-OMeTAD surface, we additionally inserted a 50 nm interlayer of PEDOT:PSS by spraying an alcoholic (dry) solution of PEDOT:PSS onto the surface of the Spiro-OMeTAD with heating (50 °C) to drive off the solvent rapidly. This allowed deposition of the PEDOT:PSS interlayer without any temperature induced damage to either the Spiro-OMeTAD or perovskite. This interlayer provides charge extraction across the whole Spiro-OMeTAD interface and direct contact with the PEDOT:PSS in the TCA.

The current density voltage curves for cells measured under AM1.5 100 mW cm^{-2} irradiance for the best-performing devices contacted using the TCA-laminate and thermally evaporated Au can be seen in **Figure 5**. Cells illuminated through the conventional FTO glass direction are said to be forward illuminated (Fwd) and cells illuminated from the TCA-laminate side, reverse illuminated (Rev). The average cell characteristics are included in **Table 1** for identically prepared batches of 12 cells of each type.

Whilst the average performance of the gold cells is marginally better than the TCA (due to higher Fill Factor (FF) and V_{OC}) the results obtained for the TCA are remarkably promising in terms of overall performance. The TCA-laminate cells suggest a good match between the PEDOT:PSS and the Spiro-OMeTAD and EIS measurements revealed no resistive or capacity barriers in these cells compared to the precious metal contact based cells. The decrease in FF can be attributed to the increased series resistance from the addition of the PEDOT:PSS and TCA layers. However, the higher J_{SC} values show the current collecting properties of the TCA to be more than adequate. In particular, the very low sheet resistance of the Epigem Ni mesh (1.2 Ω sq^{-1}) indicates that there is considerable promise

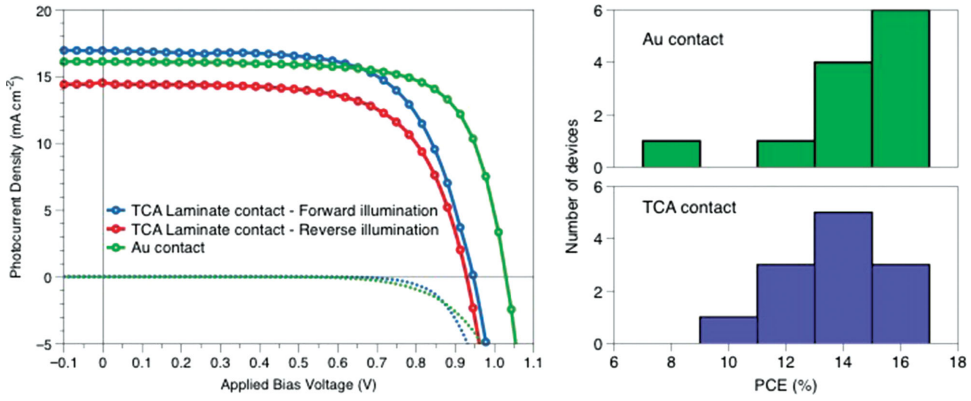

Figure 5. J–V data for typical organic-inorganic lead halide perovskite solar cells fabricated using the TCA-laminate or evaporated Au as top contact. The legend shows cell type. Also shown are the histograms demonstrating data spread.

Table 1. Solar cell performance parameters.

Back Contact	Illumination Direction	V_{OC} (V)	J_{SC} (mA cm^{-2})	Fill Factor (%)	Efficiency (%)
Au	Fwd	1.04 (0.02)	17.5 (1.8)	73.0 (7.7)	14.3 (2.2)
TCA Laminate	Fwd	0.95 (0.03)	20.7 (1.2)	63.6 (5.0)	13.3 (1.8)
TCA Laminate	Rev	0.93 (0.02)	13.9 (1.3)	67.7 (6.4)	9.8 (1.7)

Solar cell performance parameters are the average and standard deviation (s.d) values of a batch of 12 identically processed $CH_3NH_3Pb_{3-x}Cl_x$ perovskite solar cells

for making larger devices with low resistive losses. The slight voltage drop in TCA PSC devices is likely to originate from imperfect electrical contact between the Spiro-OMeTAD and the PEDOT:PSS which is an important area of future development.

When compared with forward illuminated TCA-laminate devices, the average performance of reverse illuminated cells had lower J_{SC}. The decrease in J_{SC} is not due to the transmission losses from the TCA-laminate since the transmission of the FTO coated glass and blocking layer (which light travelling in the forward direction must pass through) is similar to the transmission of the TCA-laminate, as shown in supplementary Figure S2. The transmission loss is likely to be in part caused by absorption of light by Spiro-OMeTAD at wavelengths below 427 nm (Figure S2). This filters some photons below 427 nm that would otherwise contribute to photocurrent generation within the active layer. The integrated solar spectrum between 300 to 450 nm is only equivalent to 3.9 mA cm^{-2}, which cannot fully account for the current difference between forward and reverse illumination. There may however be additional losses due to differences in the charge collection efficiency from front to back illumination.[22] The reduced average J_{SC} in rev illumination leads to a lower current flow which in turn, due to the series resistance corrections, results in an increase in the FF.

The champion cell data here shows the similar pattern with the Au contact with the best V_{OC} (1.05V) and FF (0.76) compared to the laminate V_{OC} (0.98) and FF (0.70) but with the laminate having the better J_{SC} (21mA cm^{-2}*cf* 19mA cm^{-2}). Hence the forward illuminated champion cell efficiency here was 16.7% for the Au contact and 15.5% for the laminate.

In summary, the data presented in this initial study has shown that the TCA-laminate is a simple low cost alternative to a gold evaporated contact. It can be used in standard forward illuminated conditions with the perovskite cell mounted on conducting glass or in a reverse set up which would be suitable for metal electrodes in flexible devices. Further work is in progress to examine Spiro-OMeTAD replacement/removal as this component is not only expensive but also the principal key reason that the reverse illuminated cells do not perform with higher efficiency. The TCA-laminate is indium and silver free and as such is not only low cost but is stable in the presence of any residual free halide from the perovskite. Currently we are examining PEDOT:PSS and emulsion ratios further, expanding the range of TCA deposition methods and examining the UV stability and barrier properties for moisture ingress essential for making durable devices. This work is the first phase of unlocking the incredible potential of perovskite solar cells as a high efficiency printed alternative on flexible metal foils offering simple low cost roll to roll manufacturing.

Experimental Section

Device Fabrication: To fabricate the TCA a commercially available PEDOT:PSS blend (EL-P3145 AGFA) and acrylic microemulsion pressure sensitive adhesive (F46 Styccobond) were mixed in wet quantities relating to the amount of each being present in the final dried film. The PEDOT:PSS and PSA wet solution have a solids content quoted at 0.8 and 60% respectively and a density of 1g cm^{-3}. The two were mixed such that the final volume fraction of the PEDOT:PSS in the dry TCA film was 0.0175. This mix was then tape cast onto sheets of commercially available flexible microgrid sheets (Epimesh 300 from Epigem) at a wet film thickness of 90 μm. The wet films were dried for 15 minutes at 60 °C followed by 5 minutes at 120 °C leaving final dried TCA films of 29 μm thick. To make the organolead halide perovskite photovoltaic solar cells FTO glass had a compact layer of TiO_2 deposited by spin-coating a weakly acidic solution containing 0.25 mM titanium (IV) isopropoxide in ethanol. The layer was then sintered at 500 °C for 30 minutes on a hotplate before slowly cooling to room temperature. The resulting layer thickness of the dense TiO_2 coating is approximately 50 nm. An Al_2O_3 porous scaffold was deposited by spin-coating a suspension of <50 nm Al_2O_3 nanoparticles in isopropanol before drying at 150 °C for 30 minutes. A perovskite precursor solution containing methylammonium iodide and $PbCl_2$ (3:1 molar ratio) was spin coated onto the Al_2O_3 scaffold and annealed on a hotplate at 100 °C for 90 minutes in a <0.1 ppm O_2 and H_2O atmosphere. The hole transport layer (HTL) was deposited by spin-coating a solution containing 2,2′,7,7′-tetrakis-(*N*,*N*-di-*p*-methoxyphenyl-amine)-9,9′-spirobifluorene (Spiro-OMeTAD) onto the perovskite surface. For non-laminate cells Au was evaporated onto the HTL layer using a Kurt J. Lesker Nano 36. TCA-laminate cells had a solution of PEDOT:PSS (Heraeus GSD1330S propylene glygol based 'dry' PEDOT) mixed with ethanol and isopropanol in a 1:1:1 ratio by volume sprayed onto the HTL surface whilst the cell was held on a 50 °C hotplate and left for 10 seconds post spraying. This left a layer of PEDOT:PSS approximately 50 nm thick. The TCA-laminate fabricated as described above is then laminated onto the PEDOT:PSS surface of the cells using finger pressure.

Cell Characterization: Cells were tested for their current density voltage (J-V) response on the day of fabrication. I-V testing was done using an Abet 2000 solar simulator with a KG5 filter and a Keithley 2400 source meter. The cells were scanned from forward bias to short-circuit at a scan rate of 0.15 V s^{-1}. A metal aperture mask was employed with an open area of 0.0625 cm^{-2} to define the active area of the solar cell.

To test the bulk conductivity of the TCA film a TCA was fabricated and cured as described previously onto a separate non-conducting soda glass substrate. Four 1 mm wide silver contacts were then sputtered onto the surface of the TCA at 10 mm intervals using a Quorum 150T. Samples had their thickness measured using a Dektak 150 Profilometer. A Kelvin four point probe method was then used to determine the conductivity. Optical transparency measurements were conducted using

a Perkin Elmer Lamda 750s with a 60 mm integrating sphere. Tack measurements were carried out as per the ASTM D3121 standard rolling ball tack test.

Supporting Information

Supporting Information is available from the Wiley Online Library or from the author.

Acknowledgements

This work was supported by the Engineering and Physical Sciences Research Council and the Technology Strategy Board through the SPECIFIC Innovation and Knowledge Centre (grant numbers EP/I019278/1, EP/K000292/1, EP/L010372/1)and the Welsh Government for support to the Sêr Solar programme. We would like to acknowledge funding by the European Social Fund (ESF) through the European Union's Convergence programme administered by the Welsh Government. We also acknowledge useful discussions with Brian O'Regan regarding cell measurement methods.
Note: The affiliation for Dr. M. Wijdekop was corrected on November 20, 2014, after initial publication online.

Received: August 27, 2014
Published online: September 25, 2014

[1] M. M. Lee, J. Teuscher, T. Miyasaka, T. N. Murakami, H. J. Snaith, *Science.* **2012**, *338*, 643.
[2] H.-S. Kim, C.-R. Lee, J.-H. Im, K.-B. Lee, T. Moehl, A. Marchioro, S.-J. Moon, R. Humphry-Baker, J.-H. Yum, J. Moser, M. Graetzel, N.-G. Park, *Sci. Rep.* **2012**, *2*, 1.
[3] M. J. Carnie, C. Charbonneau, M. L. Davies, J. Troughton, T. M. Watson, K. Wojciechowski, H. Snaith, D. A. Worsley, *Chem. Commun.* **2013**, *49*, 7893.
[4] M. Liu, M. B. Johnston, H. J. Snaith, *Nature.* **2013**, *501*, 395.
[5] F. Matteocci, S. Razza, F. Di Giacoma, S. Casluci, G. Mincuzzi, T. M. Brown, A. D'Epifanio, S. Licoccia, A. Di Carlo, *Phys. Chem. Chem. Phys.* **2014**, *16*, 3918.
[6] B. E. Hardin, W. Gaynor, I.-K. Ding, S.-B. Rim, P. Peumans, M. D. McGhee, *Org. Electron.* **2011**, *12*, 875.
[7] W. Gaynor, J.-Y. Lee, P. Peumans, *ACS Nano.* **2010**, *4*, 30.
[8] C.-C. Chen, L. Dou, R. Zhu, C.-H. Chung, T.-B. Song, Y. B. Zheng, S. Hawks, G. Li, P. S. Weiss, Y. Yang, *ACS Nano.* **2012**, *6*, 7185.
[9] J. R. Greer, R. A. Street, *Acta Mater.* **2007**, *55*, 6345.
[10] T. Leijtens, G. E. Eperon, S. Pathak, A. Abate, M. M. Lee, H. J. Snaith, *Nat. Commun.* **2013**, *4*, 2885.
[11] P. Docampo, M. J. Ball, M. Darwich, G. E. Eperon, H. J. Snaith, *Nat. Commun.* **2013**, *4*, 2761.
[12] O. Malinkiewicz, A. Yella, Y. H. Lee, G. M. Espallargas, M. Graetzel, M. K. Nazeeruddin, H. J. Bolink, *Nat. Photonics.* **2013**, *8*, 128.
[13] C. Roldán-Carmona, O. Malinkiewicz, A. Soriano, G. M. Espallargas, A. Garcia, P. Reinecke, T. Kroyer, M. Ibrahim Dar, M. K. Nazeeruddin, H. J. Bolink, *Energy Environ. Sci.* **2014**, *7*, 994.
[14] J. You, Z. Hong, Y. Yang, Q. Chen, M. Cai, T.-B. Song, C.-C. Chen, S. Lu, Y. Liu, H. Zhou, Y. Yang, *ACS Nano.* **2014**, *8*, 1674.
[15] G. Y. Margulis, M. G. Christoforo, D. Lam, Z. M. Beiley, A. R. Bowring, C. D. Bailie, A. Salleo, M. D. McGehee, *Adv. Energy Mater.* **2013**, *3*, 1657.
[16] C. Beyers, S. Kirsch, P. Schocker, D. Urban, *Advanced polymer design for adhesives.* in *PSTC 30th Annu. Tech. Conf.* **2007**.
[17] M. J. Powell, *Phys. Rev. B.* **1979**, *20*, 4194.
[18] I. Benedek, M. Feldstein, in *Appl. Press. Sensitive Prod*, CRC Press, Taylor and Francis Group, **2009**.
[19] I. Benedek, in *Dev. Press. Sensitive Prod*, Taylor and Francis, **2006**, 273.
[20] T. Leijtens, I. K. Ding, T. Giovenzana, J. T. Bloking, M. D. McGehee, A. Sellinger, *ACS Nano.* **2012**, *6*, 1455.
[21] K. Wojciechowski, M. Saliba, T. Leijtens, A. Abate, H. J. Snaith, *Energy Environ. Sci.* **2014**, *7*, 1142.
[22] E. Edri, S. Kirmayer, S. Mukhopadhyay, K. Gartsman, G. Hodes, D. Cahen, *Nat. Commun.* **2014**, *5*, 3461.